https://doi.org/10.15407/ujpe67.8.619

A.T. LOBURETS,[1] S.O. ZAYIKA[2]

[1] National University "Yuri Kondratyuk Poltava Polytechnic",
Educational and Scientific Institute of Oil and Gas
(24, Pershotravnevy Ave., Poltava 36004, Ukraine; e-mail: anatollob@gmail.com)
[2] National University "Yuri Kondratyuk Poltava Polytechnic",
Educational and Scientific Institute of Information Technologies and Robotics
(24, Pershotravnevy Ave., Poltava 36004, Ukraine)

SURFACE DIFFUSION AND PHASE TRANSITIONS IN ADSORBED COPPER FILMS ON (112) TUNGSTEN FACE

An experimental study of the vapor-liquid equilibrium in a two-dimensional (2D) adsorbed Cu film on the (112)W face is performed in a wide temperature range for the first time. Critical characteristics are determined. The area of coexistence of phases is established. It is shown that the features of the "liquid–gas" phase transition in the 2D system of Cu–(112)W are similar to the transitions in three-dimensional (3D) systems of Rb and Cs. The reasons for the thermodynamic similarity of 2D and 3D metallic systems are discussed. Analytical expressions for the approximation of experimental data are proposed. They determine the limits of the existence of vapor-liquid equilibrium and allow a high-precision extrapolation to the regions of critical and triple points. The coordinates of the points on the liquid and gas branches of the binodals are determined on the basis of the analysis of diffusion-formed concentration profiles.

Keywords: metals, single crystals, surface diffusion, adsorption, vapor-liquid equilibrium, two-dimensional system, thermodynamic similarity.

1. Introduction

An important problem of natural and technical sciences is the creation of a physically accurate model of a "liquid–gas" system, which would work equally well in the entire temperature range of the existence of vapor-liquid equilibrium of individual substances or their mixtures. The direct practical application of the knowledge of the mechanisms of occurrence of phenomena typical of metal liquid phases is no less important than the fundamental interest in such knowledge. For example, low-melting metals and their alloys are used in nuclear energetics as a working fluid when creating fast neutron reactors. Methods of thermodynamics do not allow one to solve practical problems without using the results of appropriate experimental studies of the thermodynamic properties of real substances. The critical characteristics of the vast majority of metals remain unclear today with the exception of alkaline ones and mercury [1, 2]. Extremely high values of critical pressures and temperatures and the high reactivity of metals stand in the way [3]. The values of the critical characteristics of transition metals were obtained by different authors only theoretically based on idealized model representations. This information is often only evaluative, because the results depend on the authors' choice of models and hypotheses [4, 5]. There is still no complete answer to the question of their nature [6] despite the large number of publications devoted to the study of critical phenomena. There are indisputable experimental facts that do not agree well with modern theory [7]. This is most pronounced in the case of metals or mixtures of substances [8, 9]. An important feature of liquid metals and semiconductors is that they become insulators during the evaporation. A "metal–nonmetal" transition takes place in the formation of the fluid phase, which is much denser than the vapor [4, 10, 11]. It is obvious that information about the atomic location and the nature of the interaction in metallic fluids is important for understanding the mechanisms of such a transition. For example, liquid mercury at temperatures above 1361 K exists as a quasibinary heterogeneous system in the form of a nanoemulsion formed by liquid phases of mercury with different densities [10]. As a result, the boiling line on the "pressure–temperature" phase diagram splits into a loop, which is characteristic of binary mixtures. This means that there may be some uncertainty in the coordinates of the critical point under such conditions. It was emphasized in [12] that the equilibrium between the phases of liquid mercury is established rather slowly. This may be one of the reasons for the differences in the results obtained with different experimental methods.

The case of significant differences of the electronegativities of adsorbate and adsorbent is interesting in "metal–on–metal" adsorption systems. Adatoms are strongly polarized at low coverages. This is the reason for the dipole-dipole repulsion between them. Alkaline, alkaline earth, and rare earth elements can form chain structures (nanowires) on the furrowed faces (112) of W. The rarefied film has dielectric properties, but the metallization of the film begins with the coverage increase and the emergence of incoherent structures due to the mutual depolarization of the adatoms [13].

As is known, the diameter of the coexistence curve $\rho_d(T)$ in van der Waals-type systems (binodal midline) is linearly dependent on the temperature (the law of rectilinear diameter). This property is often used to determine the critical point coordinates [14, 15]. However, there are many cases of violation of this law [9]. The authors of [1] were the first to show by the experiment with Rb and Cs that the curves of vapor-liquid coexistence of alkali metals significantly differ from nonmetal ones. The middle lines of the binodals of these metals deviate from the law of rectilinear diameter. In such systems, the diameter is a line whose curvature gradually increases toward the gas branch, as it approaches the critical point in the entire temperature range under study. These effects were explained by the nature of the lateral interaction of atoms in coexisting phases. The authors of [8] built a mathematical model of phase transitions for electrolytes based on [1]. They demonstrated that the experimentally determined curves of liquid-gas coexistence of alkali metals differ significantly from the behavior of the most widely studied SF_6 system [16]. The authors of [8] concluded that the similarity of the curves of liquid-gas coexistence of metals and electrolytes is manifested in the deviation of the midline of the binodals from the straight line. The researchers explained the effect by the dominant role of a long-range Coulomb lateral interaction.

Stochastic changes in the atom environment are accompanied by the constant destruction or formation of new chemical bonds. The nature of these processes changes with changes in the temperature and density or coverage degree in 2D systems. Information about the interaction potentials and the location of atoms or molecules in coexisting phases is of importance. The influence of fluctuations on phase transitions close to the critical temperature plays a key role. However, there is still no theory describing, in a consistent way, the melting of 2D systems from a microscopic point of view, as noted in the review [17]. This problem is relevant for 3D systems [18, 19].

The first studies of the structure of ordinary liquids began with the discovery of X-ray diffraction analysis [20, 21]. However, despite the vast possibilities of modern research methods, the study of a short order in liquids is given insufficient attention.

Changes in thermodynamic conditions of metal systems are accompanied by corresponding changes in the electronic structure and the interaction of atomic and electronic subsystems. It can be argued that the systematic study of phase equilibria in relation to the lateral interaction of particles began with 2D systems. They were formed by adsorbed atoms of alkaline or alkaline earth elements on low-indexed faces of refractory metal single crystals [22–24]. At the same time, some studies showed that phase transitions in the adsorbed submonolayer films are manifested in diffusion-formed concentration distributions of adsorbed atoms [25]. The investigation of such phase transitions was facilitated by the emergence of an enough wide range of experimental technical means for studying the surface layer structure of single crystals and atoms adsorbed on such surfaces [26]. The experimental techniques based on measurements of inelastic X-ray scattering are effective in the case of 3D systems. High resolution in the investigation of supercritical metallic fluids was achieved using synchrotron X-rays [19, 27].

When studying 3D systems, thermodynamic approaches have been preferred in most experimental and theoretical works for a long time. Attempts to explain the experimental facts obtained in vapor-liquid equilibria investigations at the molecular or atomic level can be found in many works [9, 12, 28, 29]. But the problem of learning the potentials of interparticle interaction remains relevant even in 2D systems [17]. In addition, in 2D "metal–on–metal" systems, an important role is played by the long-range indirect interaction of adsorbed particles through the electron gas of the substrate [22, 23, 30]. Note that the investigation of the vapor-liquid equilibrium in 2D systems is associated with significant experimental problems. The first successful attempts to overcome these difficulties were made by Bauer and Kolaskevich [31, 32]. They were able to construct gas branches of binodals (condensation lines) and determined the corresponding thermodynamic characteristics of a number of "metal–on–metal" adsorption systems.

The purpose of our work is to determine the region of coexistence of a 2D gas and the condensed phases (Cu–(112)W system). We have created a universal mathematical structure allowing to reproduce both branches of the binodal in 2D and 3D systems with high accuracy according to experimental data. It gives also a possibility with high accuracy according to available data to perform the extrapolation to those temperature ranges, where experimental results are missing for various reasons. We were interested in the question of whether 2D and 3D metal systems can be thermodynamically similar.

Experimental studies of the vapor-liquid equilibrium in a wide range of temperatures were performed with high accuracy only for such alkali metals as Cs and Rb [1]. We obtained a full binodal based on experimental data on the 2D "metal–on–metal" system for the first time.

2. Research Methods

The purity of substances under study at the temperatures of the experiment is important to investigate the "liquid–gas" phase equilibria in 3D systems. High purity can be maintained only under ultra-high vacuum conditions (10^{-11} mbar) in the case of adsorbed submonolayer (2D) films. The (112) face of v.c.c. crystals is strongly anisotropic. It is formed by rows of atoms densely packed in the [111] direction, which are separated by furrows in the [110] direction. Diffusion is also anisotropic ($D_{[111]} \gg D_{[110]}$) on such a surface [33]. The diffusion growth of Cu films on the (112)W initially occurs layer by layer, i.e., the Stransky–Krastanov mechanism is realized [34]. The model of the Cu–(112)W adsorption system is shown in Fig. 1. The physical monolayer (zone *c*), which completely covers the face of the crystal, is formed by the first two geometric ones. The third monolayer, within which we conducted research, is shown by black discs in Fig. 1. Densely packed rows of Cu atoms are separated one from another by rows of atoms of lower layers in each monolayer *1, 2, 3*.

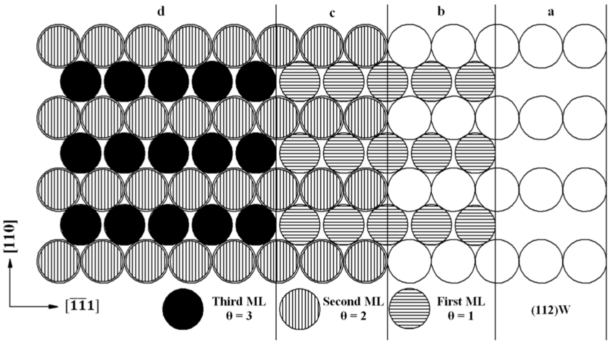

Fig. 1. Model of the (112)W face with three adsorbed Cu monolayers. (*a*) is a pure face, (*b, c, d*) are, respectively, the first, second, and third geometric monolayers of Cu (ML). The physical monolayer is formed by the first two geometric ones (zone *c*)

The distributions of adsorbed atoms served as the main source of information for constructing the Cu phase diagram (Fig. 2). They were obtained in 2D films under conditions of dynamic equilibrium in the presence of strong concentration dependences of the diffusion coefficients D and the heat of adsorption q on the coverage degree θ.

The coverage degree θ is the ratio of the number of Cu adsorbed atoms n_{Cu} to the number of adsorption centers on the surface of the adsorbent: $\theta = \frac{n_{\mathrm{Cu}}}{n_{\mathrm{W}}}$. All centers are occupied in each fully built-up geometric monolayer, so $\theta = 1$. The coverage degree is determined by the change in the local values of the work

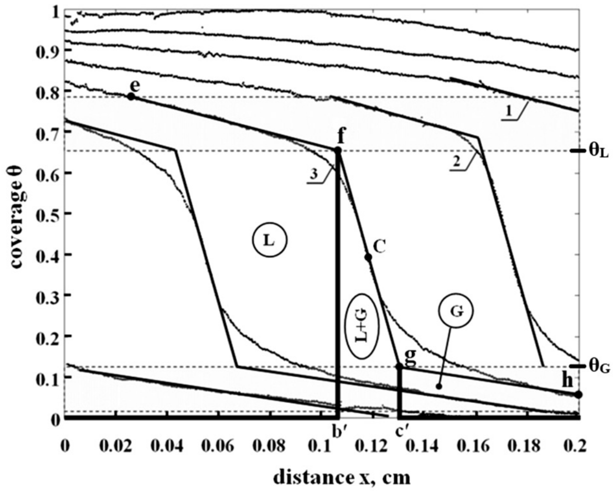

Fig. 2. The temporal displacements of the edge of the Cu adsorbed film, obtained in the third geometric monolayer (zone *d*, Fig. 1) at $T = 890$ K, carry information about the phase state of the adsorbed film. L is 2D liquid, G is 2D gas, L + G is a region of heterogeneity. $\theta = 0$ corresponds to a fully built-up physical monolayer

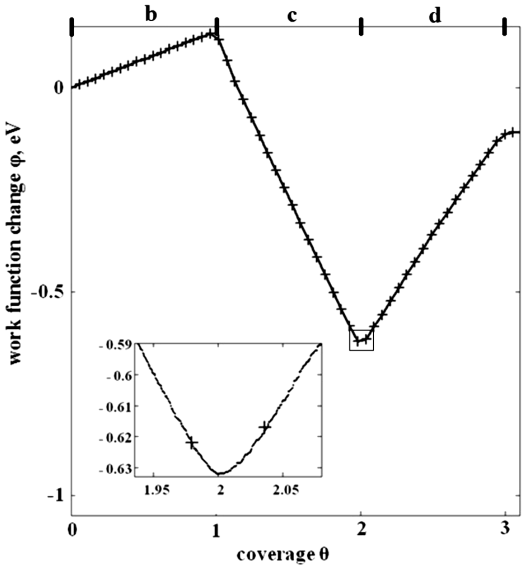

Fig. 3. Dependence of the work function on the coverage degree of Cu in the first three geometric monolayers. The inset shows the experimental local values of the work function $\phi(x)$ along the wedge in coordinates $(\theta; \phi(\theta))$

function of the face in the process of Cu diffusion and its desorption from the gas phase at a given temperature. Measurements were made after cooling the crystal to the standard temperature.

We used a scanning contact-potential (diode) microscope created by us [35] to study the Cu–(112)W system. The accuracy of measuring the coverage degree in geometric monolayers was not worse than 0.1%. The experimentally obtained calibration graph is shown in Fig. 3 presenting the change in the work function of the substrate $\phi(\theta)$ upon the sputtering of Cu with strictly calibrated portions. The work function was measured at room temperature after the heating of each new Cu portion up to 800 K. Scanning of the (112)W face of the single crystal was carried out in the [111] direction. The scanning resolution was 3.3 μm. The graph of the dependence $\phi(\theta)$ consists of segments of straight lines within the first three geometric Cu monolayers. The insert of Fig. 3 demonstrates the region formed by the experimental points, where the transition from the second geometric monolayer to the third one occurs with the formation of a sharp minimum. Still obtained these results experimentally using a wedge-shaped initial distribution with the average coverage $\theta_{\mathrm{Cu}} = 2$. The wedge was oriented in the [111] direction. The experimental results presented in the insert of Fig. 3 indicate that the effects of W face defects are almost not manifested on the distributions $\theta(x)$ due to the screening of their potentials by a physical Cu monolayer.

The linearity of the dependences $\phi(\theta)$ is a sign of the presence of the first-order phase transitions in the Cu geometric monolayers [34]. This means that the size of the islands of the condensed phase increases, as the coverage degree increases against the background of the 2D gas.

The diffusion coefficients are high at the boundary of the second and third geometric monolayers. They decrease rapidly with increasing coverage in zone d (Fig. 4). The activation energy of diffusion is minimal ($E^{\mathrm{dif}} = 0.3$ eV), but grows quickly with the coverage up to 0.93 eV [34]. The desorption heat E^{des} becomes greater from 2.41 eV to 3.33 eV in the first half of the third monolayer and remains almost unchanged in the second one (Fig. 5).

The adsorption heat was determined by the method of discrete isothermal desorption. When calculating the desorption rate, it was assumed that it remained unchanged within short time intervals (the average value was determined).

To determine the coverage degree of the equilibrium liquid θ_{L} and gas θ_{G} phases, we identified three concentration zones on each of the experimentally obtained concentration profiles of Cu $\theta_{\mathrm{Cu}}(x)$: ef, fg, and gh (Fig. 2). Within them, the coverage gradients θ_{Cu} remain constant over time. The coverage degrees θ_{L} and θ_G are determined by the coordinates of points f and g in Fig. 2. Invariance over time of the angles of inclination of segments ef, fg, and gh indicates the establishment of a dynamic equilibrium in the system. At the same time, the rate of displacement over time of points f, C, and g remains unchanged.

A large area of the gas phase G with a small concentration gradient (gh zone in Fig. 2) is formed on the substrate surface over time due to the fast diffusion at $\theta \geq \theta_{\mathrm{L}}$ and intense Cu desorption at low coverages $\theta \leq \theta_{\mathrm{G}}$. The zone ef corresponding to the condensed phase L is separated from the zone gh by a heterogeneous zone L + G with a high concentration gradient. Desorption is controlled by the Cu diffusion in the region of the heterogeneous state of the adsorbed film, i.e., by the velocity of entry of the substance into the zone of intense desorption $\theta \leq \theta_{\mathrm{G}}$. The process becomes stationary ($J_{\mathrm{des}} = J_{\mathrm{dif}}$) because of the competition between the desorption from the gas phase (desorption flow J_{des}) and the diffusion into the desorption zone from the condensed phase $\theta \geq \theta_{\mathrm{L}}$ (diffusion flow J_{dif}). The magnitude of the desorption flow is determined by the surface area occupied by the 2D gas phase under conditions of dynamic equilibrium. Concentration distributions retain their shape after each heating of the crystal in such regime. The film becomes homogeneous, and the desorption occurs evenly over the entire surface of the crystal at temperatures above the critical one. Note that the concentration region with the coexistence of L + G phases has macroscopic sizes on the concentration distributions (Fig. 2). It reaches about 0.025 cm at a temperature of 890 K. The zone of the 2D gas phase is stretched by about 0.16 cm.

The temporal changes of the coordinate x of the center C of the zone L + G are graphically represented in Fig. 6 at different temperatures. All experimental points fit well the straight lines. The velocity R of displacement of the concentration front (regions of the coexistence of L + G phases) is determined by the tangents of the inclination angles of these lines. The dependence of the logarithms of the velocities on the inverse temperature is shown in the insert. As can be seen, the process is activated, and the Arrhenius equation gives the value $E = 2.66$ eV. The uniform motion of the heterogeneity zone is maintained due to the substance flows through it into the desorption zone. The process is determined by the energy of activation of the diffusion in the gas phase and the energy of desorption from this phase. These parameters were defined by us earlier [34,36]. Assuming that $E = E_{\mathrm{G}}^{\mathrm{dif}} + E_{\mathrm{G}}^{\mathrm{des}}$, we find $E = 0.3 + 2.41 = 2.71$ eV. The difference is only 1.9%.

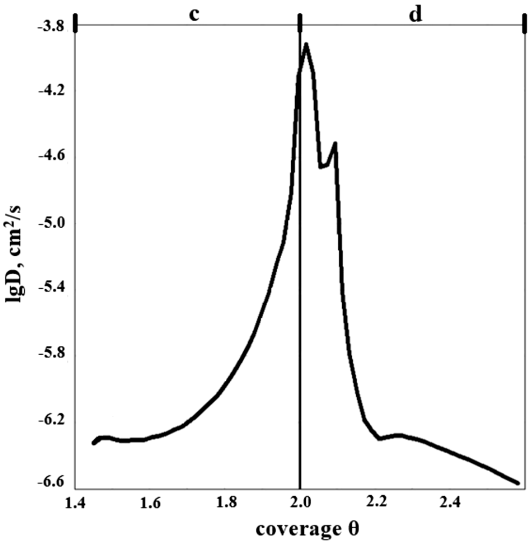

Fig. 4. Dependence of the diffusion coefficients on θ_{Cu} at the boundary of the second and third geometric monolayers at $T = 857$ K

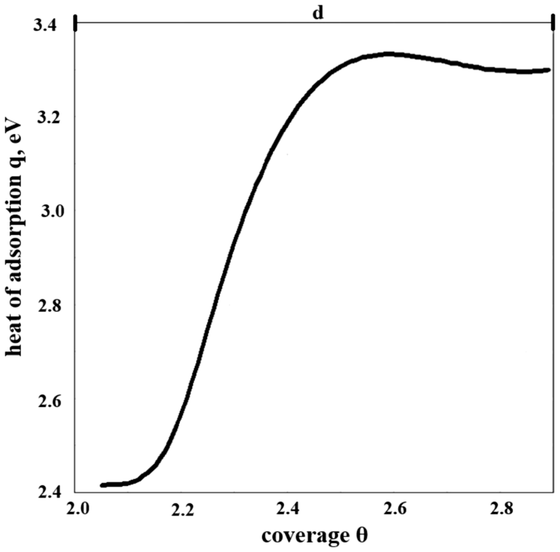

Fig. 5. The adsorption heat in the first half of the third monolayer increases by almost 1 eV. The $q(\theta)$ dependence was obtained by the method of isothermal desorption

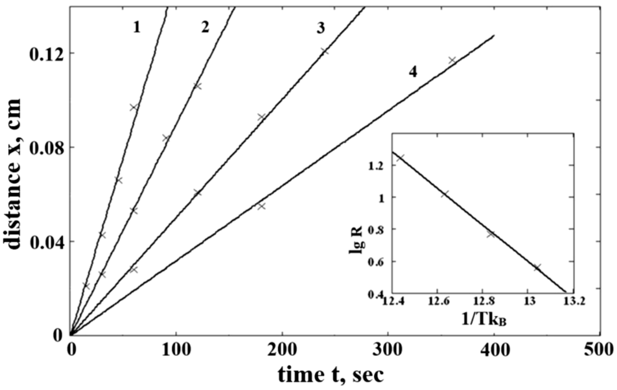

Fig. 6. Dependences of the displacement of the Cu concentration fronts on time which are obtained at different temperatures: T = 933 K (*1*); T = 919 K (*2*); T = 904 K (*3*); T = 890 K (*4*). The inset shows the Arrhenius graph

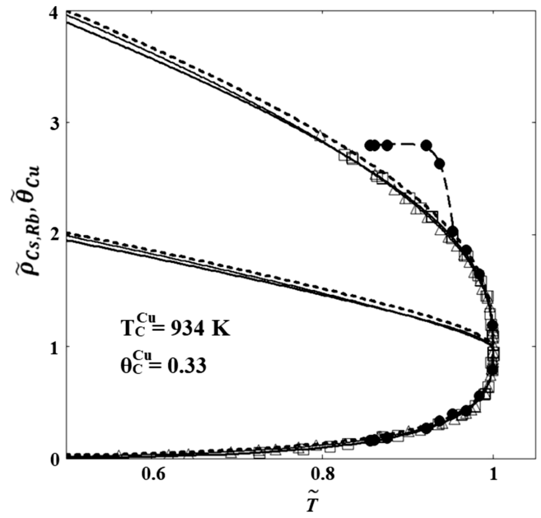

Fig. 7. Lines of vapor-liquid equilibrium calculated by us for Cs (solid thin line), Rb (thick solid line) and Cu on the (112)W face (dashed line) are presented in reduced coordinates. Formulas (1) and (2) were used to construct the Cs and Rb binodals based on the experimental results [1] (triangles and squares, respectively). The values of the critical parameters of Cu determined by us are indicated in the figure. Our experimental points are shown as black discs

We used our specially developed analytical expressions (1) and (2) to approximate the experimental data concerning the dependence of the densities of coexisting phases on the temperature. They reproduce well both branches of the binodal according to experimental data. This allows us to extrapolate experimental data to triple and critical points inclusive. The critical temperature value is a result of the extrapolation. We have

$$\theta_{\rm L} = \frac{\theta_{\rm BL}}{2} + \left(\theta_{\rm CL} - \frac{\theta_{\rm BL}}{2}\right)\frac{T}{T_{\rm C}} + \frac{\theta_{\rm BL}}{2} \times$$
$$\times \left(1 - \frac{T}{T_{\rm C}}\right)^{\beta_L + \left(1 - \frac{T}{T_{\rm C}}\right) D_{\rm L}}, \tag{1}$$
$$\theta_{\rm G} = \frac{\theta_{\rm BG}}{2} + \left(\theta_{\rm CG} - \frac{\theta_{\rm BG}}{2}\right)\frac{T}{T_{\rm C}} - \frac{\theta_{\rm BG}}{2} \times$$
$$\times \left(1 - \frac{T}{T_{\rm C}}\right)^{\beta_G + \left(1 - \frac{T}{T_{\rm C}}\right) D_{\rm G}}. \tag{2}$$

Only such standard individual thermodynamic characteristics of substances as the critical temperature $T_{\rm C}$, the critical coverage $\theta_{\rm C}$ (critical density $\rho_{\rm C}$), the Boyle coverage (density), $\theta_{\rm B}$ and $\rho_{\rm B}$, respectively, and the critical index β are used in the above dependences. A parameter D is new, which is equal to zero for the liquid phase (L). For the gas phase (G), D is close to zero in the case of inert gases. It depends on the geometry of molecules and the nature of the interaction of molecules or atoms.

All the above-mentioned parameters are considered as fitting. The sum of the least squares of the deviations of the approximation line from the experimental points was used as a criterion for evaluating the approximation results. The step-by-step regression analysis algorithm is applied.

The results of the approximation of experimental data, borrowed by us from [1] for Rb and Cs, indicate a high efficiency of the proposed method. Unlike the fundamental equations of state, our equations are universal and do not contain a large number of fitting coefficients [16] devoid of physical meaning.

3. Research Results and Discussion

The binodals of three thermodynamic systems are shown in Fig. 7 in the reduced coordinates $\tilde{\theta}_{\rm Cu} = \theta/\theta_{\rm C}$, $\tilde{\rho}_{\rm Cs,Rb} = \rho/\rho_{\rm C}$, $\tilde{T} = T/T_{\rm C}$. Thus, we investigate the 2D Cu–(112)W adsorption system and two 3D ones involving Cs and Rb [1]. As can be seen from Fig. 7, the gas and liquid branches of all three systems are located very close to one another, i.e., all three considered systems are thermodynamically similar.

The coverage degree in the condensed phase becomes equal to one at $T < 875.5$ K ($\tilde{T} \approx 0.94$) (the film reproduces the structure of the substrate). This is accompanied by a sharp reduction of the diffusion coefficients, and the evolution of the region of the concentration distribution $\theta(x)$, which corresponds to the region, where the crystalline and gas phases coexist, obeys the diffusion law.

The midlines $(\rho_L + \rho_G)/2$ demonstrate a smooth increasing curvature with a temperature rise in the whole range of reduced temperatures, i.e., the law of rectilinear diameter is violated [1, 7, 8].

The authors [4,5,8] explained the reason for the differences in "liquid-gas" phase transitions in the case of alkali metals in comparison with inert gases by the existence of a long-range Coulomb interaction in metal pairs. It takes place due to the cold ionization of atoms under the influence of high pressures in the region of the critical point. The problem of partial ionization of atoms during the adsorption and metallization of adsorbed submonolayer films was studied much more thoroughly in the case of the adsorption of metals on metals [13, 22, 23, 30].

There is no long-range order in liquids. But, with a change in thermodynamic conditions, there is also a change in the number of nearest neighbors in the coordination spheres. Multiparticle correlations of different nature arise in liquids and interact with one another. Fluctuating dynamic superstructures are formed, as the temperature increases [37]. The concept of structure becomes multidimensional for liquids. It includes not only information about the coordinates and the interaction of an individual atom with its neighbors in different coordination spheres, but also about the laws of mutually agreed (cooperative) motions of particles.

A dynamic self-organization of the diffusion zone is observed in the Cu film because of the imposition of diffusion and desorption processes. The intensity of the latter strongly depends on the coverage degree. This leads to the formation of separate areas corresponding to different phase states of the film. In fact, such a process can be considered as a manifestation of the 2D reactive diffusion. The formation of 2D phases with a certain stoichiometry and short-range structure in the liquid phase is a result of the reaction of the adsorbate with the substrate [38].

The cooperative effects become visible clearly in the dynamic properties of adsorbed films. The experimental study of that kind of effects still remains a rather difficult task in terms of a technical implementation. The main problem is the difficulty of registering such multiparticle effects as the motion of crowdions, oscillations of a nonlinear localized mode, and recombination of interstitial atoms and vacancies. This is due to the huge speeds of the processes, which makes their study almost impossible in real experiments [39].

The formation of low-gradient areas on diffusionally formed concentration profiles (self-organization of the film) in the region of high coverage can be explained by the occurrence of solitons in the 2D adsorbed film [25, 35, 37, 39]. If adatoms can form domain walls, disproportionate to the substrate (topological solitons), then the diffusion coefficients increase due to the high mobility of solitons. The efficiency of collective mechanisms is strongly suppressed by the boundaries of coexisting phases in heterogeneous systems [37, 39]. This is a zone with a high concentration gradient in the Cu film, where the gas phase flows through the dispersed condensed one are present.

4. Conclusions

The phase effects in the Cu surface diffusion on the (112)W face are very strong. The growth kinetics of the 2D phases is determined by the velocities of surface diffusion and desorption which depend on the coverage degree. This is manifested in the dynamical self-organization of the diffusion zone. The largest surface area in the diffusion zone will belong to the phases that, at this temperature, provide the most efficient transport of adsorbed atoms. This effect is a result of the implementation of collective diffusion mechanisms in the condensed phase.

The experimental study of the vapor-liquid equilibrium in a 2D adsorbed film is performed for the first time in a wide temperature range. The experimental part of the work is based on the analysis of Cu concentration profiles on the (112)W face. Such distributions were formed in the presence of a dynamic equilibrium in the adsorption system with strong differences in the diffusion coefficients and adsorption heats in the coexisting phases. We obtained the direct confirmation of the determining role of cooperative effects in the surface diffusion in the "metal–on–metal" adsorption system.

Critical characteristics (critical temperature and critical coverage) are experimentally determined in the adsorbed film. The area of coexistence of the condensed and gas phases is established in a wide temperature range.

It is shown that the thermodynamic features of the "liquid–gas" phase transition in the 2D Cu–(112)W system are similar to those discovered by the authors [1, 8] in 3D systems of alkali metals (Rb and Cs). There is a significant deviation of the midline of the binodal from the rule of rectilinear diameter. The monotonic increase of the curvature with the temperature is almost identical in all three systems in the reduced coordinates. The reasons for the thermodynamic similarity of binodals are the peculiarities of the Coulomb interaction of atoms in the gas phases and the metallization processes during the formation of condensed phases in the 2D Cu–W(112) system and in the considered 3D ones.

1. S. Jungst, B. Knuth, F. Hensel. Observation of singular diameters in the coexistence curves of metals. *Phys. Rev. Lett.* **55**, 2160 (1985).
2. F. Hensel, G.F. Hohl, D. Schaumloffel, W.C. Piligrim. Empirical regularities in the behaviour of the critical constants of fluid alkali metals.*Zeitschrift fur Physikalische Chemie* **214**, 823 (2000).
3. A. Schmon, K. Aziz, G. Pottlacher. Density determination of liquid metals by means of container less techniques. *Metallurgical and Materials Transactions A* **46**, 2674 (2015).
4. A.A. Likal'ter. Critical points of the condensation in Coulomb systems. *Usp. Fiz. Nauk* **170**, 831 (2000).
5. L.K. Alexander, A.L. Khomkin, A.S. Shumikhin. The thermodynamics and transport properties of transition metals in critical point. *High Temp. – High Pres.* **46**, 367 (2017).
6. D.Yu. Ivanov. *Critical Behavior of Nonidealized Systems* (Fiznatlit, 2003) [ISBN: 5-9221-0319-9].
7. L.A. Bulavin, V.L. Kulinskii, N.P. Malomuzh. Singularity of binodal diameter in entropy–temperature terms for atomic and molecular liquids. *Ukr. J. Phys.* **55**, 1282 (2010).
8. Y.C. Kim, M.E. Fisher. Singular coexistence-curve diameters: Experiments and simulations. *Chem. Phys. Lett.* **414**, 185 (2005).
9. J. Wang, M.A. Anisimov. Nature of vapor-liquid asymmetry in fluid criticality. *Phys. Rev. E* **75**, 051107 (2007).
10. F. Hensel. The Metal-nonmetal transition in fluid mercury: Landau-Zeldovich revisited. *Metal-to-Nonmetal Transitions* **132**, 23 (2010).
11. A.L. Khomkin, A.S. Shumikhin. Critical points of metal vapors. *JETP* **121**, 521 (2015).
12. F. Hensel, J. Jortner. The role of clustering in the liquid-vapor transition of mercury. *Z. Phys. Chem.* **228**, 329 (2014).
13. I.N. Yakovkin. Metallicity of atomic wires. *Appl. Surf. Sci.* **252**, 6127 (2006).
14. S. Reif-Acherman. The history of the rectilinear diameter law. *Quim. Nova* **33**, 2003 (2010).
15. S.M. Walas. *Phase Equilibria in Chemical Engineering* (Univ. of Kansas, 1985) [ISBN: 5-03-001106-4].
16. C. Guder, W. Wagner. Reference equation of state for the thermodynamic properties of Sulfur Hexafluoride (SF6) for temperatures from the melting line to 625 K and pressures up to 150 MPa. *J. Phys. Chem. Ref. Data* **38**, 33 (2010).
17. V.N. Ryzhov, E.E. Tareyeva, Yu.D. Fomin, E.N. Tsiok. Berezinskii–Kosterlitz–Thouless transition and two-dimensional melting. *Physics-Uspekhi* **60**, 9 (2017).
18. G.A. Martynov. The functional theory of fluids. *Teplofiz. Vysok. Temper.* **56**, 353 (2018).
19. K. Maruyama, H. Endo, H. Hoshino, F. Hensel. Void structure and intermediate-range fluctuations in the metal-nonmetal transition range in expanded liquid Hg. *Phys. Rev. B* **80**, 014201 (2009).
20. P. Debye, H. Menke. Bestimmung der inneren struktur von ussigkeiten mit rontgenstrahlen. *Physikal. Zeits* **31**, 797 (1930).
21. E.L. Meyer, W. Ramm. Die struktur der rayleigh-strahlung. *Physikalische Zeitschrift* **33**, 270 (1932).
22. A.G. Naumovets. Adsorption of alkali and other electropositive metals. *Surface and Interface Science* **5**, 157 (2016).
23. O.M. Braun, V.K. Medvedev. The interaction of particles adsorbed on the surface of metals. *Usp. Fiz. Nauk* **157**, 631 (1989).
24. A. Fedorus, D. Kolthoff, V. Koval, I. Lyuksyutov, A. Naumovets, H. Pfnur. Phase transitions in the adsorption system Li/Mo(112). *Phys. Rev. B* **62**, 2852 (2000).
25. A.G. Naumovets, Yu.S. Vedula. Surface diffusion of adsorbates. *Surf. Sci.* Rep. **4**, 365 (1985).
26. D.P. Woodruff, T.A. Delchar. *Modern Techniques of Surface Science* (Cambridge Univ. Press,1994) [ISBN: 5-03-001129-3].
27. M. Inui, D. Ishikawa, K. Matsuda, K. Tamura, A.Q.R. Baron. Experimental techniques of high-resolution inelastic X-ray scattering measurements for supercritical metallic fluids at high temperature and high pressure using synchrotron radiation at SPring-8. *Conden. Mat. Phys.* **53**, 83 (2008).
28. Y. Waseda. *The Structure of Non-Crystalline Materials: Liquids and Amorphous Solids* (McGrawnïSHill, 1980) [ISBN: 9780070684263, 007068426X].
29. M.W. Pestak, R.E. Goldstein, M.H.W. Chan, J.R. de Bruyn, D.A Balzarini, N.W. Ashcroft. Three – body interactions, scaling variables, and singular diameters ln the coexistencecurves of fluids. *Phys. Rev. B* **36**, 599 (1987).
30. J. Sliwinski, M. Wiejak, J. Kolaczkiewicz, I.N. Yakovkin. Indirect interaction in Ag and Pd adsorbed layers on the Mo(112) surface. *Appl. Surf. Sci.* **265**, 615 (2012).

31. J. Kolaczkiewicz, E. Bauer. Temperature dependence of the work function of adsorbate covered metal surfaces: a new method for the study of two-dimensional phase transitions. *Phys. Rev. Lett.* **53**, 485 (1984).
32. E. Bauer. Phase transitions in metals on metals. *Appl. Surf. Sci.* **51**, 71 (1990).
33. A.T. Loburets, N.B. Senenko, A.G. Naumovets, Yu.S. Vedula. Surface diffusion of strontium on the molybdenum (112) plane. *Phys. Low-Dim. Struct.* **10/11**, 49 (1995).
34. A.T. Loburets. Surface diffusion and phase transitions in copper overlayers on the (112) surfaces of molybdenum and tungsten. *Metallofiz. Noveishie Tekhnol.* **2**, 47 (1999).
35. A.T. Loburets. An experimental technique for recording adsorbate surface concentration profiles based on local measurements of the contact potential. *Metallofiz. Noveishie Tekhnol.* **21**, 43 (1999).
36. S.A. Zaika, A.T. Loburets, A.G. Naumovets. *The Proceedings of 1-st International conference 'Nanomaterials: Applications and Properties (NAP-2011)'* (Sumy State University, 2011).
37. I.F. Lyuksyutov, A.G. Naumovets, V.L. Pokrovsky, *Two-Dimensional Crystals* (Academic Press, 1980) [ISBN: 0124605907].
38. Yu.S. Vedula, A.T. Laburets, I.F. Lyuksyutov, A.G. Naumovets, V.V. Poplavskii. Surface diffusion and interaction of adsorbed particles of electropositive elements on refractory metals. *Kinet. Kataliz* **31**, 315 (1990).
39. O.M. Braun, Y.S. Kivshar. *The Frenkel-Kontorova Model. Concepts, Methods, and Applications* (Springer, 2004) [ISBN: 3540407715].

Received 16.07.21

А.Т. Лобурець, С.О. Заїка

ПОВЕРХНЕВА ДИФУЗІЯ І ФАЗОВІ ПЕРЕХОДИ В АДСОРБОВАНИХ ПЛІВКАХ МІДІ НА ГРАНІ (112) ВОЛЬФРАМУ

Вперше у широкому температурному діапазоні виконано експериментальне дослідження парорідинної рівноваги у двовимірній (2D) адсорбованій плівці Cu на грані (112)W. Визначено критичні характеристики. Встановлено область співіснування фаз. Показано, що особливості фазового переходу "рідина–газ" у 2D Cu–(112)W є аналогічними переходам у тривимірних (3D) системах Rb і Cs. Обговорено причини термодинамічної подібності 2D і 3D металічних систем. Запропоновано аналітичні вирази для апроксимації експериментальних даних. Вони визначають межі існування парорідинної рівноваги та дозволяють з високою точністю здійснювати екстраполяцію в області критичної та потрійної точок. Координати точок на рідинній і газовій вітках бінодалей було визначено на основі аналізу дифузійно сформованих концентраційних профілів.

Ключові слова: метали, монокристали, поверхнева дифузія, адсорбція, парорідинна рівновага, двовимірна система, термодинамічна подібність.